ISSN 1063-4576, Journal of Superhard Materials, 2014, Vol. 36, No. 4, pp. 279–287. © Allerton Press, Inc., 2014.

PRODUCTION, STRUCTURE, PROPERTIES

Crystal Structures, Elastic Properties, and Hardness of High-Pressure Synthesized CrB_2 and CrB_4[1]

S. Wang[a, b, c], X. Yu[b], J. Zhang[b], Y. Zhang[a], L. Wang[a], K. Leinenweber[d], H. Xu[b], D. Popov[e], C. Park[e], W. Yang[e, f], D. He[c], and Y. Zhao[a, b, *]

[a] *HiPSEC & Physics Department, University of Nevada, Las Vegas, NV 89154, USA*
[b] *LANSCE & EES Divisions, Los Alamos National Laboratory, Los Alamos, NM 87545, USA*
[c] *Institute of Atomic & Molecular, Physics, Sichuan University, Chengdu 610065, P. R. China*
[d] *Deptartment of Chemistry and Biochemistry, Arizona State University, Tempe, AZ 85287, USA*
[e] *HPCAT & HPSynC, Geophysical Laboratory, Carnegie Institution of Washington, Argonne, Illinois 60439, USA*
[f] *Center for High Pressure Science and Technology Advanced Research (HPSTAR), Shanghai 201203, P.R. China*
**e-mail: Yusheng.Zhao@UNLV.edu*

Received April 10, 2014

Abstract—Chromium tetraboride (CrB_4), a recently proposed candidate for superhard materials, has been synthesized at high pressure and temperature by a solid-state reaction. As a byproduct, chromium diboride (CrB_2) also forms and co-exists with CrB_4 in the final product. The comparative studies of crystal structure, elastic property, and hardness of both phases have been conducted at the same sample environment conditions. The crystal structure of CrB_4 has been refined with an orthorhombic symmetry of *Immm* (space group no. 71) or *Pnnm* (space group no. 58) using X-ray diffraction data. Further simulations indicate that the structural distinction between *Immm* and *Pnnm* can be resolved by neutron diffraction, due to the high scattering cross-section of boron (^{11}B) by neutrons. Although CrB_2 and CrB_4 have close bulk modulus at about 230 GPa, the measured asymptotic Vickers hardness yields 16 GPa for CrB_2 but 30 GPa for CrB_4, which is nearly two times that of CrB_2. The dramatic enhancement in hardness in CrB_4 is attributed to the strong three-dimensional Cr–B network, in contrast to the layered lattice structure of hexagonal CrB_2.

DOI: 10.3103/S1063457614040066

Keywords: chromium borides, CrB_4, CrB_2, high-pressure synthesis, structure, compressibility, superhard material.

1. INTRODUCTION

Incorporation of small, light, and covalent elements, such as B, C, and N, into the crystalline lattices of large, electron-rich transition metals (e.g., W and Re) holds the promise to produce a new class of super- or ultra-hard materials that are more cost-effective and versatile than traditional superhard materials of diamond and cBN [1–6]. Since 2007, inspired by frontier research on ReB_2 by Chung et al. [7], there has been a new surge of research interest in searching for ultra-incompressible and superhard transition-metal (TM) borides, nitrides, and carbides. These efforts have led to a series of new system including diborides (ReB_2 [8–10] and RuB_2 [10]), tetraborides (WB_4 [11, 12], FeB_4 [13], MnB_4 [14, 15], and CrB_4 [16–18]), nitrides (Re_xN [19] and WN_x [20]), and carbides (Re_2C [21]). Among them TM tetraborides (TMB_4) are of particular interest because they often exhibit superior hardness over their diboride, nitride, and carbide counterparts, primarily due to their high boron content and associated three-dimensional (3D) covalent network [22].

Because of the experimental difficulties associated with the synthesis of phase–pure TM borides, the crystal structure and intrinsic hardness of TMB_4 continue to be a subject of debate [23, 24]. However, increasing experimental evidence indicates that hexagonal WB_4, the hardest TM boride known to date, has an asymptotic (i.e., load-independent) Vickers hardness of $H_V = 30$ GPa [10–12], which is close to those of pure γ-boron (~ 30 GPa) and β-boron (~ 26 GPa) but not in that superhard regime [25]. In addition, due to their layered stacking along the *c*-axis of alternating TM layers and B dimers, hexagonal TM tetraborides are structurally unfavorable to form mechanically isotropic superhard materials [22]. A similar atomic stacking configuration also occurs in most TM diborides with hexagonal crystal symmetries, for examples, *P*6/*mmm* (S.G.

[1] The text was submitted by the author(s) in English.

no. 191) in TiB_2 and $P6_3/mmc$ (S.G. no. 194) in ReB_2 [1, 6]. As pointed out by Wang et al. [22], the hardness of hexagonal TMB_4 is predominantly determined by the covalently B–B bonded network between the intercalated boron dimers in the parent lattice of transition metals. From this point of view, the primary role that TM lattice plays is a "place–holder" for boron dimers, which limits the hardness of hexagonal TMB_x to the level of elemental boron and boron–rich compounds with asymptotic $H_V \approx 26–30$ GPa [25, 26]. However, after an exhausting search of the known structures for TMB_x, the orthorhombic TMB_4 (TM = Cr, Mn, and Fe) is found to exhibit a 3D bonding network between TM and boron [15, 17, 27], which is structurally more favorable than hexagonal TMB_4 for producing mechanically isotropic borides. As expected, recent reports show that the orthorhombic FeB_4 and MnB_4 possess a superior nanoindentation hardness of 62 GPa and a Vickers hardness of $H_V = 37.4$ GPa under a load of 9.8 g [13, 14], approaching the superhard regime as defined by the asymptotic $H_V \approx 40$ GPa. Strikingly, both borides also exhibit intriguing superconducting and magnetic properties [13, 14, 16] .

Chromium tetraboride, CrB_4, was first synthesized in 1962 [27] and has recently been reemerged as a promising candidate for achieving superhardness [16–18]. However, the synthesis of single-phase CrB_4 is still challenging because CrB_2 often co-exists as a secondary phase in the final product, indicating that CrB_2 is thermodynamically more stable in the Cr–B system [17, 18]. In addition, the detailed structure of CrB_4 is an unsettled issue between orthorhombic symmetries of *Immm* and *Pnnm* [17]. A similar structure controversy has also been reported in MnB_4 [14, 28]. In this work, for the first time, we synthesized CrB_4 through a solid-state reaction between chromium and boron under high-pressure (p)/high-temperature (T) conditions. The final product was characterized by powder X-ray diffraction (XRD), high-p diamond-anvil cell (DAC) compression experiments, and Vickers hardness measurements.

2. EXPERIMENTAL DETAIL

Commercially available chemical pure Cr (> 99.9% purity) and B (> 99.9% purity) powders in a molar ratio Cr : B = 1 : 4.5 were homogenously mixed for the synthesis of CrB_4. Excessive boron was used to eliminate the possible CrB_2 byproduct. High p-T synthetic experiments were carried out in a multianvil cubic press at the Arizona State University, USA. Pressure and temperature generation and calibration were described previously [29]. A prepressed pellet of the starting mixture was placed in a hexagonal boron nitride (hBN) capsule, which served as a high-pressure sample chamber and was surrounded by a graphite heater for in situ high temperature. Experimental details are described elsewhere [29].

The final product was characterized by powder X-ray diffraction with copper target. The crystal structures of borides were refined using the Rietveld method with the GSAS software [30]. The Vickers hardness was measured using a Micromet–2103 hardness tester on the well-sintered bulk sample at 25–1000 g loading force and a 15 s dwelling time.

High pressure synchrotron X-ray diffraction (XRD) experiments using the diamond-anvil cell (DAC) were performed at the HPCAT 16BM–D beamline of the Advance Photon Source (APS), Argonne National Laboratory. The boride powder was loaded into the sample hole in a stainless steel gasket pre–indented to 30 micron thick with neon as the pressure–transmitting medium. A few ruby balls were also loaded in the same sample chamber to serve as the internal pressure standard [31]. The sample was compressed up to 20 GPa at room temperature. The two-dimensional angle–dispersive XRD patterns were collected with focused monochromatic X-rays with wavelength 0.41325 Å and a Mar3450 imaging plate. The program Fit2D was used to integrate all 2D images into one-dimensional diffraction profiles [32] .

3. RESULTS AND DISCUSSION

Figure 1a shows the XRD pattern of the experimental run product synthesized at 14 GPa and 1200°C for 45 min. CrB_4 and CrB_2 are identified as major phases in the recovered sample at ~ 45% and ~ 50% mole fractions, respectively. About 5% hBN originated from BN sample container is also detected. Even though a 12.5% excess of boron was used in the starting material to prepare CrB_4, CrB_2 still formed as a major byproduct under the present experimental conditions. However, the unreacted boron left behind in the final product cannot be detected by X-ray diffraction (Fig. 1a), indicating an amorphous state. The similar phenomenon has also been found previously in the synthesis of ReB_2 and WB_4 [9, 11]. For synthesis at atmospheric pressure, recent studies show that a prolonged heating duration of 8–14 days can increase the phase fraction of CrB_4 to as high as 90% [17, 18], indicating that CrB_2 may be an intermediate phase formed in advance of CrB_4. Obviously, the

formation of CrB_4 is kinetically sluggish at atmospheric pressure. Although the heating time is short in our high-*p* synthesis (i.e., only 45 min), the obtained CrB_4 has a moderate fraction of 45% in the recovered sample, indicating that the formation of CrB_4 is kinetically more favorable at high pressure. However, our later synthesis shows that CrB_4 does not form at all at a lower pressure of 8 GPa and temperature of 1200°C for 1 hour, which is similar to the case of FeB_4 with reported formation pressures of 8–18 GPa [13]. But for MnB_4, it can be synthesized at a lower pressure of 3 GPa [14].

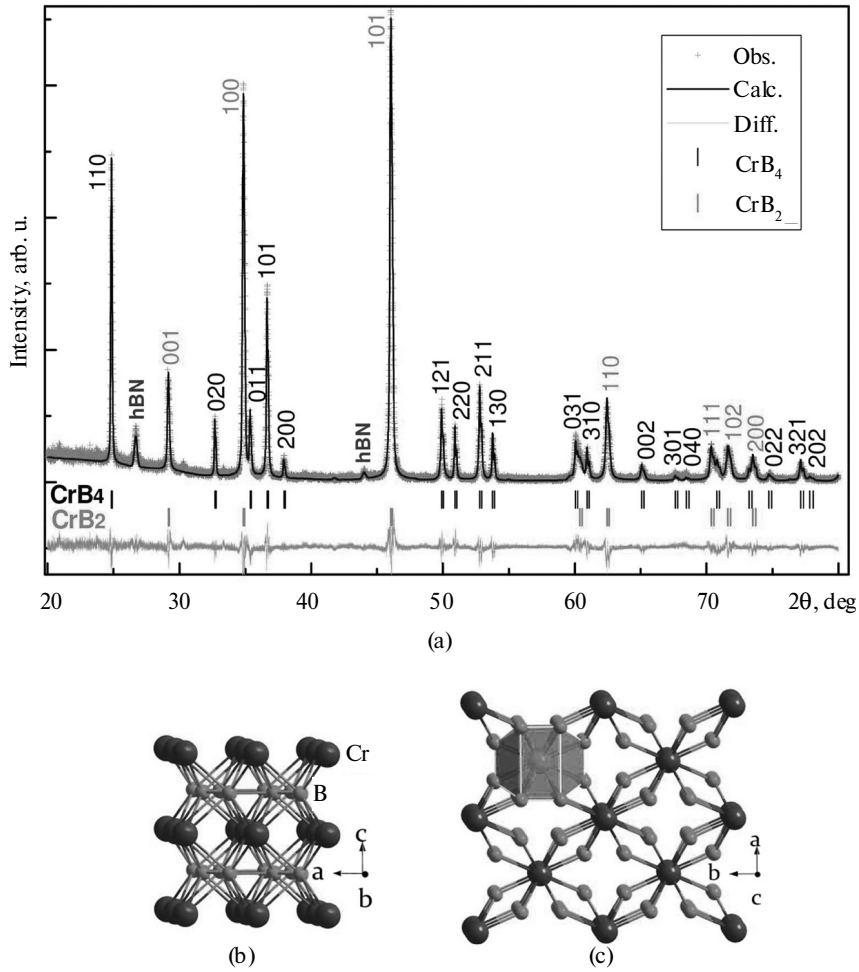

Fig. 1. (a) Rietveld analysis of powder X-ray diffraction pattern of co-existing CrB_2 and CrB_4 phases. The sample was synthesized at 14 GPa and 1200°C for 45 min. Crosses and black lines represent the observed and calculated profiles, respectively. The difference curve between the observed and calculated profiles is shown in light gray. The peak positions of Bragg reflections for CrB_4 and CrB_2 are tick marked. Impurity phase hBN originates from the capsule material used for high pressure synthesis. (b) Polyhedral view of the structures of CrB_2 (left, 2 × 2 × 2 unit cell) and CrB_4 (right, 2 × 2 × 2 unit cell) (c).

As shown in Fig. 1a, the refined structure of CrB_2 is hexagonal with space group *P*6/*mmm* (no. 191), a symmetry typical for many metal diborides [1]. The refined lattice parameters are $a = 2.9747$ (2) Å and $c = 3.0660$ (2) Å, which agree well with the reported values [16–18]. The details of the refined structural parameters are summarized in the Table. A subset of Bragg peaks in Fig. 1a can be indexed in terms of orthorhombic phase, which belongs to crystalline CrB_4. The structural refinements were thus performed using an earlier proposed symmetry of *Immm* (no. 71). The obtained lattice parameters are $a = 4.7481$ (1) Å, $b = 5.4815$ (3) Å, and $c = 2.8662$ (2) Å (see the table for details), which is consistent with the recent studies [16–18]. The corresponding structures of CrB_2 and CrB_4 are shown in Fig. 1b and 1c in polyhedral views. Evidently, the Cr and B ions in CrB_4 are covalently bonded to form a strong 3D network, similar to that in MnB_4 [28]. In contrast, the Cr–B bonds in CrB_2 are two-dimensional from the layer-structured stacking sequence, which leads to lower hardness as discussed below. Based on electron diffraction measurements, a new space group, *Pnnm* (no. 58), has recently been proposed for CrB_4 [17], which is selected in this work as the structural candidate

for refinement. However, within the resolution of our XRD data, the refined results using *Pnnm* are indistinguishable from those using *Immm*, as reflected by the similar refinement agreement indices (see the table).

Summary of the refined structural parameters for CrB_2 and CrB_4

	CrB_2	CrB_4	
p, T conditions	Ambient conditions		
Space group	*P6/mmm* (no. 191)	*Immm* (no. 71)	*Pnnm* (no. 58)
Cell content	CrB_2	Cr_2B_8	Cr_2B_8
a_0, b_0, c_0, Å	2.9747 (2), 3.0660 (2)	4.7481 (1), 5.4815 (3), 2.8662 (2)	4.7483 (2), 5.4817 (3), 2.8663 (2)
Cell volume, $Å^3$	23.501	74.584	74.585
ρ, $g \cdot cm^{-3}$	5.202	4.241	4.241
Cr positions	1*a*, (0, 0, 0)	2*a*, (0, 0, 0)	2*c*, (0, 0, 0)
B positions	2*d*, (1/3, 2/3, 1/2)	8*n*, (0.191, 0.350, 0)	4*g*, (0.1640, 0.6351, 0) 4*g*, (0.2236, 0.3210, 0)
R_{wp}, %, R_p, %, χ^2	8.6, 6.2, 4.1		8.4, 6.3, 4.0

To better illustrate the distinction between the two space groups of CrB_4, the powder X-ray and neutron diffraction patterns are simulated for *Pnnm* and *Immm*, which are shown in Figs. 2a, 2b. The corresponding structures are depicted in Figs. 2c, 2d. Evidently, a major difference between the two structures is the atomic

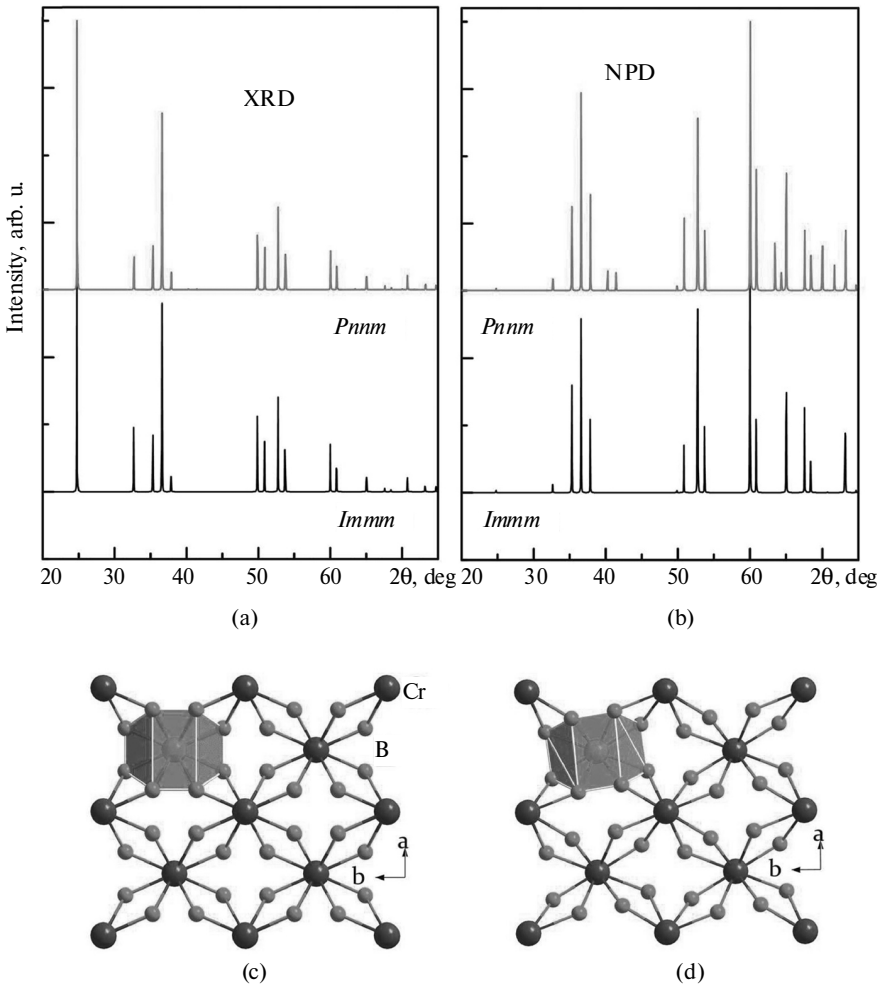

Fig. 2. (a) Simulated powder X-ray and (b) neutron diffraction patterns for CrB_4 based on two possible structures of *Immm* (no. 71) and *Pnnm* (no. 58). (c) Crystal structures of *Immm* and *Pnnm* (d) (see the table for structure details).

positions of boron with the lower–symmetry *Pnnm* structure having tilted [CrB_{12}] coordination (Figs. 2c, 2d). Since boron is a light element and has a small X-ray scattering factor, the structural distinction between *Pnnm* and *Immm* cannot be resolved by X-ray diffraction due to the small scattering cross–section of boron atoms. By contrast, the neutron scattering cross–section of an element does not scale with its atomic number, and neutrons are more sensitive to the presence of light elements (e.g., boron) in a crystal structure. As illustrated in Fig. 2b, the *Pnnm* and *Immm* structures can be readily distinguished by neutron diffraction (NPD), because some additional peaks for the low–symmetry structure *Pnnm* phase that are hard to discern in its XRD pattern are much stronger in the neutron pattern. Hence, further neutron diffraction measurement on $Cr^{11}B_4$ is warranted to resolve the structural controversy.

Phase stability and compressibility of CrB_4 were investigated by synchrotron X-ray diffraction in a diamond-anvil cell (DAC). Figure 3 shows the selected XRD patterns collected under room-temperature compression. Because both CrB_4 and CrB_2 exist in the sample, it allows us to conduct a comparative study of the two phases with exactly the same sample environments. The results show that CrB_2 and CrB_4 are structurally stable up to 25 GPa, and no phase transition was observed. The derived pressure–volume data for CrB_2 and CrB_4 are fitted to the second order Birch–Murnaghan equation of state [33], as shown in Fig. 4. The obtained bulk moduli, B_0, for CrB_2 and CrB_4 are 228(5) GPa and 232(6) GPa, respectively, which agree well with the results of first-principles calculations [28, 34]. The obtained bulk moduli are close to the boron-rich compounds, such as $B_{13}N_2$ [35], B_6O [36], and B_4C [37]. In spite of the fact that CrB_2 and CrB_4 have a nearly identical bulk modulus, they show different behaviors in the axial compressibility as illustrated in Fig. 5. For CrB_2, the *c*–axis is significantly more compressible than the *a*-axis (Fig. 5a), which is consistent with its layered atomic stacking along *c*-axis (Fig. 1b). For CrB_4, as shown in Fig. 5b, the compression along the three crystallographic axes is more isotropic than in CrB_2. Interestingly, the *b*-axis is the least compressible although it has the largest lattice parameter (5.481 Å), whereas the most compressible axis, the *c* axis, corresponds to the shortest lattice parameter ($c = 2.866$ Å), which are in agreement with the recent results of first-principles simulations [28]. This anomalous compressive behavior has only sparsely been reported [20], and is likely to be associated with the peculiar atomic arrangements in orthorhombic CrB_4.

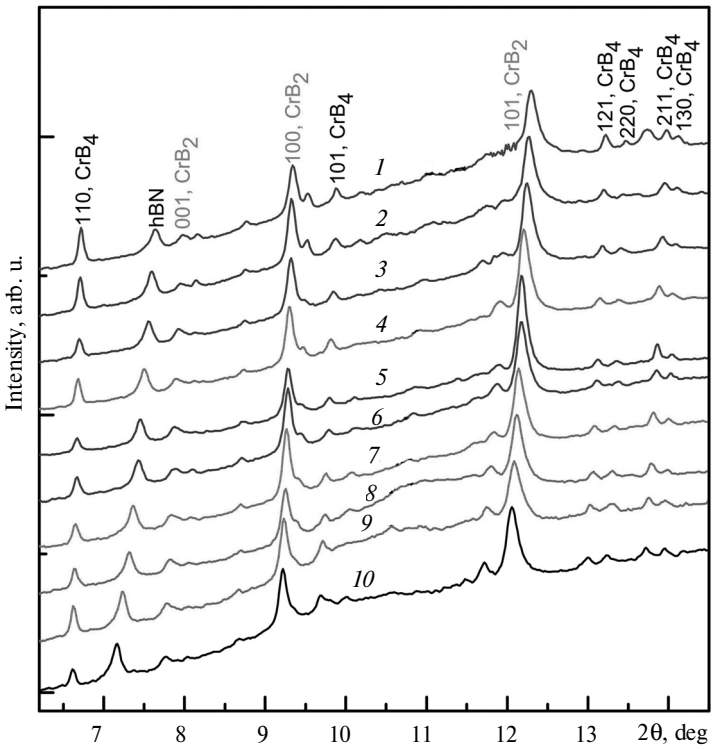

Fig. 3. Selected high-pressure synchrotron X-ray diffraction patterns collected at room temperature in a diamond–anvil cell: 15.7 (*1*), 13.6 (*2*), 12.0 (*3*), 10.2 (*4*), 8.9 (*5*), 7.7 (*6*), 5.8 (*7*), 4.5 (*8*), 2.8 (*9*), 1.4 (*10*) GPa. The incident X-ray wavelength is $\lambda = 0.41326$ Å.

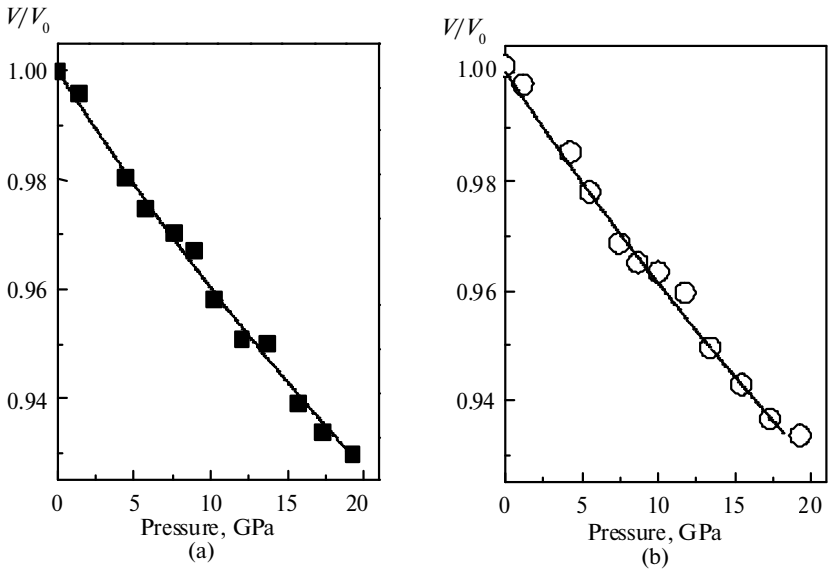

Fig. 4. Volume–pressure data fitted to the second order Birch–Murnaghan equation of state for (a) CrB_2 and (b) CrB_4.

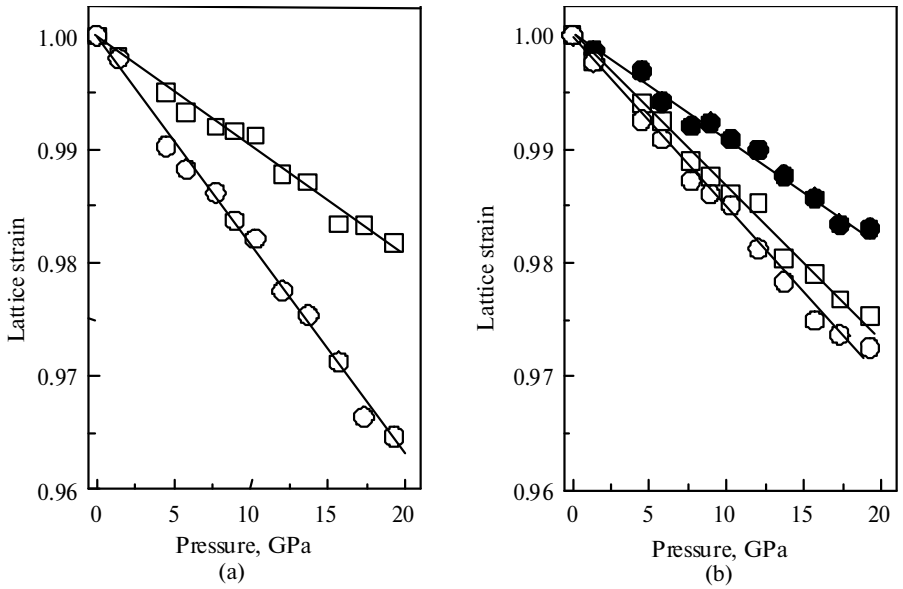

Fig. 5. Relative cell parameters as a function of pressure for (a) CrB_2 and (b) CrB_4 derived from high-pressure X-ray diffraction data. (□) a/a_0, (○) c/c_0, (●) b/b_0.

Vickers hardness measurements were performed on the recovered bulk sample with mixed phases of CrB_2 and CrB_4. Figure 6 shows a typical fluorescence image from the polished sample surface, which was taken using the microscopy system of the hardness tester with a magnification of ×400. Clearly, CrB_4 and CrB_2 are distinguishable by dark and bright regions, respectively, allowing their indentation measurements to be conducted on each of the two boride phases. As shown in Fig. 7, the determined asymptotic hardness of CrB_4 is ~ 30 GPa, which is close to that of the known hardest WB_4 and is presumably attributed to its strong 3D Cr–B bonding network. However, the layer–structured CrB_2 has a substantially lower hardness of ~ 16 GPa, which agrees with the previously reported value [3].

4. CONCLUSIONS

In summary, for the first time, we synthesized the orthorhombic CrB_4 phase at high p-T conditions at 14 GPa and 1200°C through a solid–state reaction between chromium and boron elements. The only byprod-

uct is CrB_2, which may be an intermediate phase prior to the formation of CrB_4. Despite a short heating time of 45 minutes in the high-p synthesis, the phase mole fraction of CrB_4 in the final product yields a high fraction value of 45%, indicating accelerated formation kinetics of CrB_4 at high p-T condition. The refined crystal structures of CrB_2 and CrB_4 are hexagonal $P6/mmm$ and orthorhombic $Immm$ or $Pnnm$, respectively. Our simulations indicate that the major structural difference between $Immm$ and $Pnnm$ is the atomic positions of boron rendering neutron diffraction a more effective approach to resolve these two structures. Based on high-p synchrotron XRD experiment, the obtained bulk moduli of CrB_2 and CrB_4 are 228 GPa and 232 GPa, respectively. Despite the similar bulk moduli, CrB_4 has a much higher asymptotic Vickers hardness of ~ 30 GPa than that of CrB_2 (~ 16 GPa), which is presumably attributed to the strong three-dimensional Cr–B network in CrB_4.

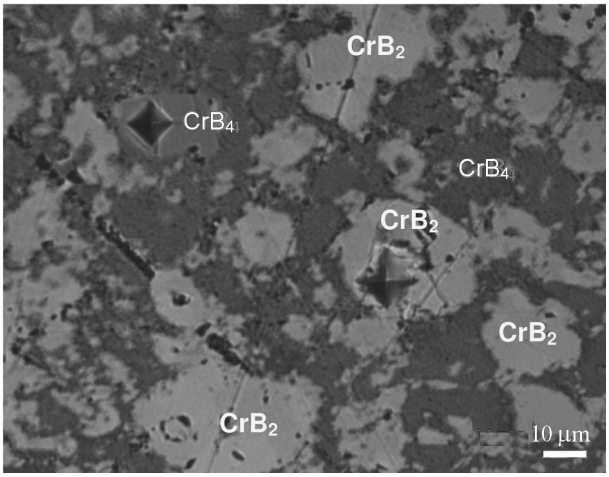

Fig. 6. A florescence image of the indentations produced at an indenter tip load of 200 g with a dwell time of 15 s. The dark and bright regions are CrB_4 and CrB_2, respectively.

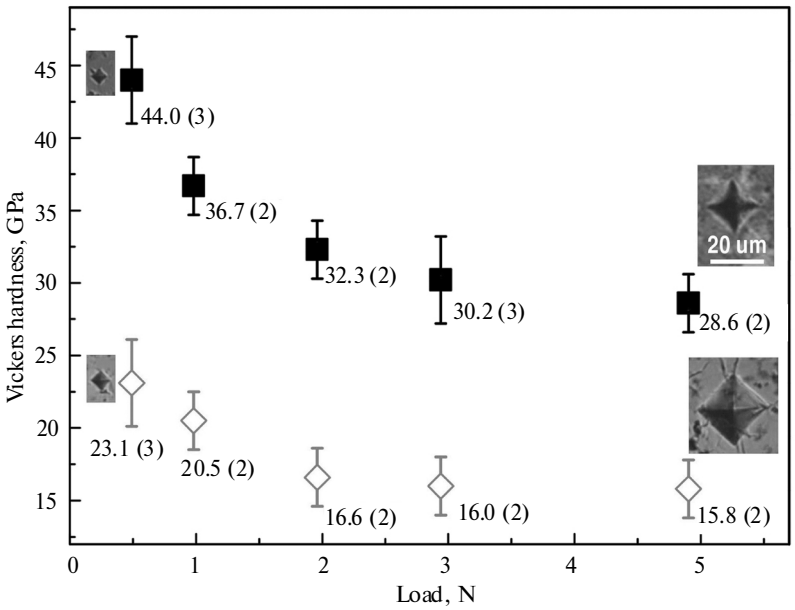

Fig. 7. Vickers hardness of CrB_4 (solid squares) and CrB_2 (open diamonds)as a function of indenter tip load. Insets are the selected images of indentation.

Portions of this work were performed at HPCAT, Advanced Photon Source (APS), Argonne National Laboratory. HPCAT operations are supported by DOE-NNSA under Award no. DE-NA0001974 and DOE-BES under Award no. DE-FG02-99ER45775, with partial instrumentation funding by NSF. APS is supported by DOE-BES, under Contract no. DE-AC02-06CH11357. This work is also supported by UNLV High Pressure Science and Engineering Center (HiPSEC), which is a DOE NNSA Center of Excellence operated under

Cooperative Agreement DE-FC52-06NA27684, and UNLV start-up funding to Y. Zhao. This research is partially supported by Los Alamos National Laboratory, which is operated by Los Alamos National Security LLC under DOE Contract DE-AC52-06NA25396. HPSynC is supported as part of EFree, an Energy Frontier Research Center funded by DOEBES under Grant DE-SC0001057.

REFERENCES

1. Ivanovskii, A.L., The search for novel superhard and incompressible materials on the basis of higher borides of *s, p, d* metals, *J. Superhard Mater.*, 2011, vol. 33, no. 2, pp. 73–87.
2. Veprek, S., Zhang, R.F., and Argon, A.S, Mechanical properties and hardness of boron and boron-rich solids., *Ibid.*, 2011, vol. 33, no. 6, pp. 409–420.
3. Zachary, Z., New superhard ternary borides in composite materials, In New Superhard Ternary Borides in Composite Materials, Metal, Ceramic and Polymeric Composites for Various Uses, Cuppoletti, J., Ed, *Int. Tech*, 2011, pp. 61–78.
4. Brazhkin, V.V., Lyapin, A.G., and Hemley, R.J., Harder than diamond: Dreams and reality, *Philos. Mag. A*, 2002, vol. 82, no. 2, pp. 231–253.
5. Brazhkin, V., Dubrovinskaia, N., Nicol, M., Novikov, N., Riedel, R., Solozhenko, V., and Zhao, Y., From our readers: What does 'harder than diamond' mean? *Nature Mater.*, 2004, vol. 3, no. 9, pp. 576–577.
6. Pierson, H.O., In Handbook of refractory carbides and nitrides: properties, characteristics, processing, and applications, Westwood, NY: Noyes Publications, 1996.
7. Chung, H.-Y., Weinberger, M.B., Levine, J.B., Kavner, A., Yang, J.-M., Tolbert, S.H., and Kaner, R.B., Synthesis of ultra-incompressible superhard rhenium diboride at ambient pressure, *Science*, 2007, vol. 316, no. 5823, pp. 436–439.
8. Dubrovinskaia, N., Dubrovinsky, L., and Solozhenko, V.L., Comment on "Synthesis of ultra-incompressible superhard rhenium diboride at ambient pressure", *Ibid.*, 2007, vol. 318, no. 5856, p. 1550.
9. Qin, J., He, D., Wang, J., Fang, L., Lei, L., Li, Y., Hu, J., Kou, Z., and Bi, Y., Is rhenium diboride a superhard material? *Adv. Mater.*, 2008, vol. 20, no. 24, pp. 4780–4783.
10. Gu, Q., Krauss, G., and Steurer, W., Transition metal borides: superhard versus ultra-incompressible, *Ibid.*, 2008, vol. 20, no. 19, pp. 3620–3626.
11. Mohammadi, R., Lech, A.T., Xie, M., Weaver, B.E., Yeung, M.T., Tolbert, S.H., and Kaner, R.B., Tungsten tetraboride, an inexpensive superhard material, *Proc. Nat. Acad. Sci.*, 2011, vol. 108, no. 27, pp. 10958–10962.
12. Mohammadi, R., Xie, M., Lech, A.T., Turner, C.L., Kavner, A., Tolbert, S.H., and Kaner, R.B., Toward inexpensive superhard materials: tungsten tetraboride-based solid solutions, *J. Am. Chem. Soc.*, 2012, vol. 134, no. 51, pp. 20660–20668.
13. Gou, H., Dubrovinskaia, N., Bykova, E., Tsirlin, A.A., Kasinathan, D., Schnelle, W., Richter, A., Merlini, M., Hanfland, M., Abakumov, A.M., Batuk, D., Van Tendeloo, G., Nakajima, Y., Kolmogorov, A.N., and Dubrovinsky, L., Discovery of a superhard iron tetraboride superconductor, *Phys. Rev. Lett.*, 2013, vol. 111, no. 15, art. 157002.
14. Gou, H., Tsirlin, A.A., Bykova, E., Abakumov, A.M., Van Tendeloo, G., Richter, A., Ovsyannikov, S.V., Kurnosov, A.V., Trots, D.M., Konôpková, Z., Liermann, H.-P., Dubrovinsky, L., and Dubrovinskaia, N., Peierls distortion, magnetism, and high hardness of manganese tetraboride, *Phys. Rev. B*, 2014, vol. 89, no. 6, art. 064108.
15. Litterscheid, C., Knappschneider, A., and Albert, B., Single crystal structure of MnB_4, *Z. Anorg. Allg. Chem.*, 2012, vol. 638, no. 10, pp. 1608–1608.
16. Knappschneider, A., Litterscheid, C., Dzivenko, D., Kurzman, J.A., Seshadri, R., Wagner, N., Beck, J., Riedel, R., and Albert, B., Possible superhardness of CrB_4, *Inorg. Chem.*, 2013, vol. 52, no. 2, pp. 540–542.
17. Niu, H., Wang, J., Chen, X.-Q., Li, D., Li, Y., Lazar, P., Podloucky, R., and Kolmogorov, A.N., Structure, bonding, and possible superhardness of CrB_4, *Phys. Rev. B*, 2012, vol. 85, no. 14, art. 144116.
18. Knappschneider, A., Litterscheid, C., Kurzman, J., Seshadri, R., and Albert, B., Crystal structure refinement and bonding patterns of CrB_4: A boron-rich boride with a framework of tetrahedrally coordinated B atoms, *Inorg. Chem.*, 2011, vol. 50, no. 21, pp. 10540–10542.
19. Friedrich, A., Winkler, B., Bayarjargal, L., Morgenroth, W., Juarez-Arellano, E.A., Milman, V., Refson, K., Kunz, M., and Chen, K., Novel rhenium nitrides, *Phys. Rev. Lett.*, 2010, vol. 105, no. 8, art. 085504.
20. Wang, S., Yu, X., Lin, Z., Zhang, R., He, D., Qin, J., Zhu, J., Han, J., Wang, L., Mao, H.-K., Zhang, J., and Zhao, Y., Synthesis, crystal structure, and elastic properties of novel tungsten nitrides, *Chem. Mater.*, 2012, vol. 24, no. 15, pp. 3023–3028.
21. Zhao, Z., Cui, L., Wang, L., Xu, B., Liu, Z., Yu, D., He, J., Zhou, X., Wang, H., and Tian, Y., Bulk Re_2C: crystal structure, hardness, and ultra-incompressibility, *Cryst. Growth Des.*, 2010, vol. 10, no. 12, pp. 5024–5026.
22. Wang, M., Li, Y., Cui, T., Ma, Y., and Zou, G., Origin of hardness in WB_4 and its implications for ReB_4, TaB_4, MoB_4, TcB_4, and OsB_4, *Appl. Phys. Lett.*, 2008, vol. 93, no. 10, art. 101905.
23. Zang, C., Sun, H., and Chen, C., Unexpectedly low indentation strength of WB_3 and MoB_3 from first principles, *Phys. Rev. B*, 2012, vol. 86, no. 18, art. 180101.

24. Zhang, R.F., Legut, D., Lin, Z.J., Zhao, Y.S., Mao, H.K., and Veprek, S., Stability and strength of transition-metal tetraborides and triborides, *Phys. Rev. Lett.*, 2012, vol. 108, no. 25, art. 255502.

25. Qin, J., Nishiyama, N., Ohfuji, H., Shinmei, T., Lei, L., He, D., and Irifune, T., Polycrystalline γ-boron: As hard as polycrystalline cubic boron nitride, *Scr. Mater.*, 2012, vol. 67, no. 3, pp. 257–260.

26. Mukhanov, V.A., Kurakevych, O.O., and Solozhenko, V.L., Thermodynamic model of hardness: Particular case of boron-rich solids, *J. Superhard Mater.*, 2010, vol. 32, no. 3, pp. 167–176.

27. Andersso, S. and Lundstro, T., Crystal structure of CrB_4, *Acta Chem. Scand.*, 1968, vol. 22, no. 10, pp. 3103–3110.

28. Yang, M., Wang, Y., Yao, J., Li, Z., Zhang, J., Wu, L., Li, H., Zhang, J., and Gou, H., Structural distortion and band gap opening of hard MnB_4 in comparison with CrB_4 and FeB_4, *J. Solid State Chem.*, 2014, vol. 213, pp. 52–56.

29. Wang, W., He, D., Wang, H., Wang, F., Dong, H., Chen, H., Li, Z., Zhang, J., Wang, S., Kou, Z., and Peng, F., Research on pressure generation efficiency of 6–8 type multianvil high pressure apparatus, *Acta Phys. Sin*, 2010, 59, no 5, pp. 3107–3115.

30. Toby, B.H., EXPGUI, a graphical user interface for GSAS, *J. Appl. Cryst.*, 2001, vol. 34, pp. 210–213.

31. Mao, H.K., Xu, J., and Bell, P.M., Calibration of the tuby pressure gauge to 800 kbar under quasi-hydrostatic conditions, *J. Geophys. Res.*: *Solid Earth*, 1986, vol. 91, no. B5, pp. 4673–4676.

32. Hammersley, A.P., Svensson, S.O., Hanfland, M., Fitch, A.N., and Hausermann, D., Two-dimensional detector software: from real detector to idealized image or two-theta scan, *High Press. Res.*, 1996, vol. 14, nos. 4–6, pp. 235–248.

33. Birch, F., Finite elastic strain of cubic crystals, *Phys. Rev.*, 1947, vol. 71, no. 11, pp. 809–824.

34. Okamoto, N.L., Kusakari, M., Tanaka, K., Inui, H., and Otani, S., Anisotropic elastic constants and thermal expansivities in monocrystal CrB_2, TiB_2, and ZrB2, *Acta Mater.*, 2010, vol. 58, no. 1, pp. 76–84.

35. Kurakevych, O.O. and Solozhenko, V.L., 300-K equation of state of rhombohedral boron subnitride, *Solid State Commun.*, 2009, vol. 149, nos. 47–48, pp. 2169–2171.

36. Nieto-Sanz, D., Loubeyre, P., Crichton, W., and Mezouar, M., X-ray study of the synthesis of boron oxides at high pressure: Phase diagram and equation of state, *Phys. Rev. B*, 2004, vol. 70, no. 21, art. 214108.

37. Nelmes, R.J., Loveday, J.S., Wilson, R.M., Marshall, W.G., Besson, J.M., Klotz, S., Hamel, G., Aselage, T.L., and Hull, S., Observation of inverted-molecular compression in boron carbide, *Phys. Rev. Lett.*, 1995, vol. 74, no. 12, pp. 2268–2271.